

## COLLABORATIVE SENSING BASED WIDEBAND DETECTION IN COGNITIVE RADIO NETWORKS

<sup>1</sup>XIAOFENG JIANG, <sup>2</sup>XINGHUA LIU, <sup>3</sup>HONGSHENG XI

<sup>123</sup>University of Science and Technology of China, Department of Automation

E-mail: <sup>1</sup>[xjf@mail.ustc.edu.cn](mailto:xjf@mail.ustc.edu.cn), <sup>2</sup>[salxh@mail.ustc.edu.cn](mailto:salxh@mail.ustc.edu.cn), <sup>3</sup>[xihs@ustc.edu.cn](mailto:xihs@ustc.edu.cn)

### ABSTRACT

Spectrum sensing techniques are useful to increase spectrum utilization in a cognitive radio network by sensing spectrum holes without harmful interference. The collaboration of sensing information among cognitive radio nodes can significantly increase the reliability of spectrum sensing. Due to hardware limitation, each cognitive radio node has to sense one narrowband channel at a time. Consequently, the sensing procedure consumes a lot of time to get the sufficient information. A wideband sensing method is used to reduce the time overhead. Each node only senses a small amount of linear combinations of the information of all channels, and then transmit this low dimensional detection vector to the fusion center where the information is reconstructed. As a result, the time overhead and the communication overhead are significantly reduced. Six performance measures have been observed in the system which considers the call hold and residence of both licensed users and cognitive radio nodes. The observations show that the algorithm has a good performance.

**Keywords:** *collaboration, wideband sensing, sparse vector, subspace pursuit, detection, false alarm*

### 1. INTRODUCTION

There is a significant increase in the demand for radio spectrum with the emergence of new applications and the compelling need for mobile services in recent years. This is partly due to the increasing interest of consumers in convenient and ubiquitous wireless services, and the interest has been driving the evolution of wireless networks to high speed data networks. However, ever since the 1920s, in order to avoid the serious interference in wireless services, the wireless providers have been required to apply an exclusive license from the government. Today, it is becoming very difficult to find vacant bands to either deploy new services or to enhance the existing ones with most of the spectrum being already allocated according to former U.S. Federal Communications Commission chair William Kennard [1]. On the other hand, not every channel in every band is in use all the time. In an experiment for studying the spectrum occupancy between 30MHz and 3GHz in New York City[2], the average utilization rate during the measurement period was only 13%. A large number of vacant spectrum holes can be discovered in the spectrum which is not used. A variety of technologies have been proposed to increase the spectrum utilization. As one of these, cognitive radio (CR) has emerged as a promising technology to improve the spectrum

utilization by opportunistic utilizing wireless resources without causing harmful interference. In a CR network, the unlicensed users continuously sense the spectrum environment and transmit the data when an appropriate vacant spectrum hole is detected.

The spectrum sensing for detecting spectrum holes is the precondition for the implementation of CR networks. The existing spectrum sensing techniques have to face two main challenges: reliable sensing and wideband sensing. The hidden terminal problem [3] is the main reason that causes the unreliable sensing. Since the signals of licensed users are usually undermined by channel shadowing and multipath fading between the target under detection and CR nodes, it is generally difficult to distinguish between a white spectrum and a weak signal. An inaccurate detection result may cause harmful interference by transmitting the data in a band occupied by a licensed user. The wideband sensing is hard to be implemented for the main reason of hardware limitations. The CR nodes usually use a tunable narrowband band pass filter at the radio frequency(RF) front-end to sense one band at a time due to the costliness of a wideband RF front-end [3]. Consequently, it is a lot of time delay for detecting all channels. An efficient wideband spectrum sensing method can mitigate the



requirement of the RF front-end and maximize the opportunistic throughput of CR nodes.

Collaborative spectrum sensing techniques are proposed to improve the reliability of spectrum sensing. In a CR network, all CR nodes transmit their sensing reports to a fusion center, where the reports are merged and an accurate sensing result is obtained. Different SNR estimations and channel fading environments are considered in [4] and [5] to improve the reliability of sensing information. C. Yunfei [6] studies the optimum number of collaborative users to get the tradeoff of the reliability and the complexity. The Byzantine attacks which come from malicious users and carry false sensing data are taken into account in [7]. The cooperative sensing techniques with different mechanisms are considered in the studies of [8, 9]. However, the collaborative spectrum sensing method brings a new serious problem. The transmissions of reports have brought a lot of communication overhead, since all nodes should transmit their sensing reports which have large sizes. This problem is solved by grouping the CR nodes in the conventional method. Each group of nodes sense a small amount of narrowband channels and transmit a few reports. The performance will be reduced. This algorithm is also considered in [10].

A wideband sensing method based on subspace pursuit is proposed in this study to reduce both the time overhead and the communication overhead. Each CR node senses all channels simultaneously instead of sensing one narrowband at a time, and get a linear combination of the information of all channels. The information of channels can be reconstructed from a small amount of these linear combinations under certain conditions. Consequently, the sensing procedure can be finished in a short time with the wideband sensing method, and the size of reports can be significantly reduced. The studies of [11-14] exploit a method to solve this problem by estimating the information of all channels with only a small amount of sensing results. The sensing procedure is modeled as a partially observed Markov decision process (POMDP). Z. Qing [11] proposes this idea and a myopic sensing method. S. Ahmad [12] studies the optimality of the myopic sensing method and proves it under the conditions which are very close to practice. X. Wang [13] exploits the impact of the rate less code, W. Lingcen [14] modifies the cost function of POMDP with the switching time.

The rest of this paper is organized as follows. In section two, the detection procedure of wideband sensing based on the energy detection technique is

given. The reconstruction algorithm for the measurement information is given in section three, and multi-node collaboration for processing the measurements is developed in section four. After that, the simulation is presented in section five, and the conclusion is drawn in section six.

## 2. SYSTEM MODEL

We consider a CR network with  $M$  CR nodes that locally monitor a set of  $N$  wireless channels, and each channel is either occupied by a licensed user or idle. The states of channels are set as 1(occupied) and 0(idle). To detect the channel state, we adopt the energy detection technique which doesn't need any prior information of the licensed user. Each channel should be detected  $T$  times in a detection procedure. Consequently, a CR node should transmit a  $N \times T$  measurement matrix to the fusion center which will process  $M$  measurement matrices in conventional collaborative spectrum sensing techniques. The time overhead and the communication overhead are very large. A novel wideband sensing method based on the sparse observations of the measurement matrix is developed to overcome this problem.

### 2.1 Energy Detection

Considering the scene that the CR node  $m$  is detecting the channel  $n$ , where  $1 \leq m \leq M$  and  $1 \leq n \leq N$ , we give a detailed description of energy detection and obtain some useful parameters to measure the performance. The goal of energy detection is to decide between the following two hypotheses:

$$\begin{aligned} H_{0,m,n} : x(t, m, n) &= v(t, m, n) \\ H_{1,m,n} : x(t, m, n) &= h_{m,n}s(t, m, n) + v(t, m, n) \end{aligned} \quad (1)$$

$$t = 1, 2, \dots, T$$

where

$H_{0,m,n}$  represents the absence of the licensed user in channel  $n$ ,

$x(t, m, n)$  is the signal received by the CR node  $m$  in channel  $n$ ,

$v(t, m, n)$  is the additive white Gaussian noise(AWGN),

$H_{1,m,n}$  represents the presence of a licensed user,

$s(t, m, n)$  is the signal of a licensed user,

$h_{m,n}$  is the amplitude gain of channel  $n$ ,

$\gamma_{m,n}$  is the signal-to-noise ratio(SNR).



Let  $\mathbf{x}_{m,n}$  denote  $[x(1, m, n), x(2, m, n), \dots, x(T, m, n)]^T$ . The decision rule is given by

$$T(\mathbf{x}_{m,n}) \underset{H_{0,m,n}}{\overset{H_{1,m,n}}{\geq}} \lambda \quad (2)$$

where  $T(\mathbf{x}_{m,n})$  is the test statistic and  $\lambda$  is the test threshold.  $T(\mathbf{x}_{m,n})$  has the following distribution according to the work of Urkowitz [15].

$$T(\mathbf{x}_{m,n}) \sim \begin{cases} \chi_T^2 & \text{under } H_{0,m,n} \\ \chi_T^2(2\gamma_{m,n}) & \text{under } H_{1,m,n} \end{cases} \quad (3)$$

where  $\chi_T^2$  and  $\chi_T^2(2\gamma_{m,n})$  denote the central and non-central chi-square distributions, respectively, each with T degrees of freedom and  $2\gamma_{m,n}$  for the non-centrality parameter of the latter distribution.

The detection probability  $P_{d,m,n}$  and the false alarm probability  $P_{f,m,n}$  equal  $P\{\text{observe } H_{1,m,n} | H_{1,m,n}\}$  and  $P\{\text{observe } H_{1,m,n} | H_{0,m,n}\}$ , respectively. Then can be given by [16] in the non-fading environment where  $h_{m,n}$  is deterministic.

$$P_{d,m,n} = Q_{T/2}(\sqrt{2\gamma}, \sqrt{\lambda}) \quad (4)$$

$$P_{f,m,n} = \frac{\Gamma(T/2, \lambda/2)}{\Gamma(T/2)} \quad (5)$$

where  $\Gamma(\cdot)$  and  $\Gamma(\cdot, \cdot)$  are complete and incomplete gamma functions, respectively, and  $Q_m(\cdot, \cdot)$  is defined as the generalized Marcum Q-function

$$Q_m(a, b) = \int_b^\infty \frac{x^m}{a^{m-1}} \exp(-\frac{x^2+a^2}{2}) I_{m-1}(ax) dx \quad (6)$$

where  $I_{m-1}(\cdot)$  is the modified Bessel function.

In the fading environment where  $h_{m,n}$  is varying due to shadowing or fading,  $P_{f,m,n}$  is independent of  $\gamma_{m,n}$  since the signal of licensed user is absent under  $H_{0,m,n}$ .  $P_{d,m,n}$  can be derived by averaging over fading statistic in this case.

$$P_{d,m,n} = \int_x Q_{T/2}(\sqrt{2\gamma}, \sqrt{\lambda}) f_\gamma(x) dx \quad (7)$$

where  $f_\gamma(x)$  is the probability density function of  $\gamma_{m,n}$  under fading.

### 2.2 Wideband Detection

Considering the scene that the CR node m detects all channels  $\{1, 2, \dots, N\}$ , the node m should detect each channel T times and spend total  $N \times T$  units of time detecting all channels, or configure N filters locally to detect all channels T times simultaneously in conventional sensing techniques. Both approaches are too expensive. Frequency selective filters are equipped to detect all channels simultaneously instead of detecting a channel at a time in this study. Each CR node equips L frequency selective filters locally where L is much smaller than N, one filter can detect a linear combination of the information of all channels T times. The detection procedure can also be completed by only one filter in  $L \times T$  units of time.

The detection procedure at each CR node can be represented by a  $L \times N$  filter coefficient matrix  $\Phi$ . Let N dimensional vectors  $\mathbf{x}'_m$  and  $\mathbf{v}'_m$  represent the power and noise in channels, they equal  $[x(t, m, 1), x(t, m, 2), \dots, x(t, m, N)]^T$  and  $[v(t, m, 1), v(t, m, 2), \dots, v(t, m, N)]^T$ , respectively. The L dimensional compressive detection vector  $\mathbf{D}'_{t,m}$  can be given by

$$\begin{aligned} \mathbf{D}'_m &= \Phi \mathbf{x}'_m \\ &= \Phi(\mathbf{x}'_m - \mathbf{v}'_m) + \Phi \mathbf{v}'_m \\ &= \Phi \mathbf{s}'_m + \mathbf{e} \\ &t = 1, 2, \dots, T \end{aligned} \quad (8)$$

where  $\mathbf{s}'_m$  denotes the measurement vector of the signal of the licensed user  $\mathbf{x}'_m - \mathbf{v}'_m$ , and  $\mathbf{e}$  denotes  $\Phi \mathbf{v}'_m$ . If  $s(t, m, n)$  equals zero, the channel n is not occupied by a licensed user. The time overhead in the detection procedure is polynomial with respect to  $L \times T$  which is much smaller than  $N \times T$ .

### Notation

Here we instate some notations that are used throughout the paper. For any N dimensional vector  $\mathbf{x}$ , we write  $\|\cdot\|_p$  for the usual  $l_p$  vector

norm  $\|\mathbf{x}\|_p$  which equals  $(\sum_{n=1}^N x_n^p)^{\frac{1}{p}}$ , where  $1 \leq p \leq \infty$ , especially, we reserve  $\|\mathbf{x}\|_0$



as  $|\{i, x_i \neq 0\}|$ . We denote the columns of the matrix  $\Phi$  by  $(\phi_j)_{j \in J}$ . Further, let  $\Phi_Z$  and  $\mathbf{x}_Z$  be the submatrix and subvector with column indices  $j \in Z$  for any  $Z \subseteq J$ , respectively. Then, we define the pseudo inverse of the full rank matrix  $\Phi$  by  $\Phi^\dagger$  which is  $(\Phi^* \Phi)^{-1} \Phi^*$ .

**Filter Coefficient Matrix  $\Phi$**

We can reconstruct  $\mathbf{s}_m^t$  from  $\mathbf{D}_m^t$  if the filter coefficient matrix  $\Phi$  can ensure that k-sparse vectors are able to be distinguished based on the observation that  $\mathbf{s}_m^t$  is k-sparse. That is, we should make sure that  $\Phi$  is a linear embedding of the set of k-sparse vectors. Here, we say that a vector is k-sparse when it has  $k \leq N$  nonzero entries. Emmanuel J. Candes and Terence Tao [17] define K-restricted isometry constant  $\delta_K$  and  $K, K'$ -restricted orthogonality constant  $\theta_{K, K'}$  to be the smallest quantity such that  $\Phi$  obeys

$$(1 - \delta_K) \|\mathbf{s}_{mZ}^t\|_2^2 \leq \|\Phi_Z(\mathbf{s}_{mZ}^t)\|_2^2 \leq (1 + \delta_K) \|\mathbf{s}_{mZ}^t\|_2^2 \quad (9)$$

$$|\langle \Phi_Z(\mathbf{s}_{mZ}^t), \Phi_{Z'}(\mathbf{s}_{mZ'}^t) \rangle| \leq \theta_{K, K'} \|\mathbf{s}_{mZ}^t\|_2 \|\mathbf{s}_{mZ'}^t\|_2 \quad (10)$$

for all disjoint subsets  $Z, Z' \subseteq J$  of the cardinality at most  $K, K'$  and all real vectors  $\mathbf{s}_{mZ}^t, \mathbf{s}_{mZ'}^t$ . The numbers  $\delta_K$  and  $\theta_{K, K'}$  measure how close the vectors  $\phi_j$  are to behave like an orthogonality system. And, the orthogonality constant  $\theta_{K, K'}$  can be controlled by  $\delta_{K+K'}$  according to the lemma in [17], that is,

$$\theta_{K, K'} \leq \delta_{K+K'} \leq \theta_{K, K'} + \max(\delta_K, \delta_{K'}) \quad (11)$$

The condition  $\delta_{2k} \leq 1$  implies that the filter coefficient matrix  $\Phi$  preserves the geometry of the set of k-sparse vectors and performs like the orthogonal transformation.

Then, an important question is to find the matrix with a good 2k-restricted isometry constant. Gaussian matrix which meets the condition is easy to be constructed. We set each entry of  $\Phi$  as independent and identically distributed Gaussian random variable with mean zero and variance  $1/L$ . Because a k-sparse vector contains about  $s \log(N/s)$  bits of information,  $O(k \log(N/k))$  should be sufficient for the value of L. Here, we give two more examples: the bernoulli random matrix and the subsampled

Fourier matrix. Their restricted isometry constants obey the following conditions, respectively.

$$\delta_{2k} < \varepsilon \text{ whenever } L \geq \frac{k \log(N/k)}{\varepsilon^2}$$

$$\delta_{2k} < \varepsilon \text{ whenever } L \geq \frac{k \log^5 N \log \varepsilon^{-1}}{\varepsilon^2}$$

**3. RECONSTRUCTION OF MEASUREMENT**

It is possible to reconstruct the measurement vector  $\mathbf{s}_m^t$  from the compressive detection vector  $\mathbf{D}_m^t$  when the filter coefficient matrix  $\Phi$  stably embeds the set of k-sparse vectors. Then, we can use the decision rule of energy detection (2) to process the vector set  $\{\mathbf{s}_m^t, 1 \leq t \leq T\}$ , and obtain the accurate sensing information of all channels. The reconstruction algorithm is derived from subspace pursuit for compressive sensing signal reconstruction [18], it consists of five major steps. We first define the following parameters.

$\mathbf{D}_m^t$ : the compressive detection vector of all channels at time t.

$\mathbf{s}_m^t$ : the measurement vector of all channels at time t.

$Z_m^t$ : the indices corresponding to the k largest magnitude elements of  $\mathbf{s}_m^t$ .

$\mathbf{u}_m^t$ : the residue of  $\mathbf{D}_m^t$ .

Because the sequence of  $\{\mathbf{s}_m^1, \dots, \mathbf{s}_m^T\}$  has high self-correlation, we can let  $Z_{m0}^t$  equal  $Z_m^{t-1}$  and let  $Z_{m0}^1$  equal NULL, this operation can greatly reduce the computational overhead. With  $Z_{m0}^t$ , we can calculate the initial value of  $\mathbf{u}_{m0}^t$  which equals  $\mathbf{D}_m^t - \Phi_{Z_{m0}^t} \Phi_{Z_{m0}^t}^\dagger \mathbf{D}_m^t$ . The iterative steps of the reconstruction algorithm are given as follows.

Step 1: the correlation maximization (CM) operation is performed to discover the k largest magnitude elements of  $\Phi^* \mathbf{u}_{mi-1}^t$ , and we can discover the location of the elements which carry a lot of energy.

Step 2: the indices of elements with the higher correct probability can be determined by merging  $Z_{mi-1}^t$  and  $Z_{mi}^t$ .

Step 3: the elements of  $\mathbf{s}_m^t$  corresponding to the indices are estimated.

Step 4: the k largest magnitude entries of the estimations are chosen to update  $Z_{mi}^t$ , and the residue  $\mathbf{u}_{mi}^t$  is calculated.

Step 5: the stopping criterion is checked to determine whether the measurement vector has been approximated.

The pseudo code of the reconstruction algorithm is summarized as algorithm 1.

Algorithm 1

Input: k,  $\Phi$ ,  $\mathbf{D}_m^t$

Initial step:

$$i = 0, \mathbf{s}_m^t \leftarrow \{0\}^N$$

$$Z_{m0}^t \leftarrow NULL \text{ or } Z_{m0}^t \leftarrow Z_m^{t-1}$$

$$\mathbf{u}_{m0}^t \leftarrow \mathbf{D}_m^t - \Phi_{Z_{m0}^t} \Phi_{Z_{m0}^t}^\dagger \mathbf{D}_m^t$$

Repeat:  $i \leftarrow i + 1$

Step 1:  $Z_{mi}^t \leftarrow CM(\Phi^* \mathbf{u}_{mi-1}^t)$

Step 2:  $Z_{mi}^t \leftarrow Z_{mi-1}^t \cup Z_{mi}^t$

Step 3:  $\mathbf{s}_c \leftarrow \Phi_{Z_{mi}^t}^\dagger \mathbf{D}_m^t$

Step 4:  $Z_{mi}^t \leftarrow CM(\mathbf{s}_c)$

$$\mathbf{u}_{mi}^t \leftarrow \mathbf{D}_m^t - \Phi_{Z_{mi}^t} \Phi_{Z_{mi}^t}^\dagger \mathbf{D}_m^t$$

Step 5: if  $\|\mathbf{u}_{mi}^t\|_2 > \|\mathbf{u}_{mi-1}^t\|_2$

$$Z_{mi}^t \leftarrow Z_{mi-1}^t$$

$$\mathbf{s}_m^t \leftarrow \{0\}^N \quad \mathbf{s}_{mZ_{mi}^t}^t \leftarrow \Phi_{Z_{mi}^t}^\dagger \mathbf{D}_m^t$$

quit the iteration

Output:  $\mathbf{s}_m^t$

### Analysis of Reconstruction Algorithm

#### Correlation Maximization

The correlation maximization (CM) is the core operation throughout the reconstruction algorithm, it is performed to discover the indices of elements which carry a lot of energy in the measurement vector  $\mathbf{s}_m^t$ , but how does it work for this purpose. We first give an intuitive explanation. The ultimate goal of  $\{\phi_j \mid j \in J\}$  is to behave like an orthonormal system for sparse vectors, we can naturally set  $1+1$ -restricted isometry constant  $\delta_{1+1}$  as 0 to approximate an orthonormal system, according to (11) and the definition of  $1,1$ -restricted orthogonality constant  $\theta_{1,1}$ , we can get

$$\theta_{1,1} = 0$$

$$|\langle \Phi_{\{j\}}(\mathbf{s}_{m\{j\}}^t), \Phi_{\{j\}}(\mathbf{s}_{m\{j\}}^t) \rangle| \leq 0$$

$$\langle \Phi_{\{j\}}, \Phi_{\{j\}} \rangle = 0$$

Then, we consider  $\Phi^* \mathbf{D}_m^t$  in the noiseless environment.

$$\Phi^* \mathbf{D}_m^t = \Phi^* \Phi \mathbf{s}_m^t$$

$$= [\phi_1^* \phi_1, \phi_2^* \phi_2, \dots, \phi_N^* \phi_N]^T \mathbf{s}_m^t$$

The nonzero elements of  $\mathbf{s}_m^t$  which we want to discover carry a lot of energy in this ideal scenario, consequently, an efficient filter coefficient matrix should ensure that the CM operation can collect the indices of nonzero elements.

Then considering the unideal scenario, we denote the set of the indices of nonzero elements by  $Z_m^t$ , in the light of the definition of the CM operation and the property 1.7 of [17], we can get

$$\|\Phi_{Z_m^t}^* \mathbf{D}_m^t\|_2 \geq \|\Phi_{Z_m^t}^* \mathbf{D}_m^t\|_2$$

$$= \|\Phi_{Z_m^t}^* \Phi_{Z_m^t} \mathbf{s}_m^t\|_2$$

$$\geq \lambda_{\min}(\Phi_{Z_m^t}^* \Phi_{Z_m^t}) \|\mathbf{s}_m^t\|_2$$

$$\geq (1 - \delta_k) \|\mathbf{s}_m^t\|_2$$

where  $\lambda_{\min}$  is the minimum eigenvalue. Here, if we assume that the chosen indices set  $Z_{m1}^t$  is disjoint from  $Z_m^t$ , according to (10) and lemma 1 of [18], we can get

$$\|\Phi_{Z_{m1}^t}^* \mathbf{D}_m^t\|_2 = \|\Phi_{Z_{m1}^t}^* \Phi_{Z_{m1}^t} \mathbf{s}_m^t\|_2$$

$$\leq \delta_{2k} \|\mathbf{s}_m^t\|_2$$

Consequently, we can get the inequality that  $1 - \delta_k$  is less than  $\delta_{2k}$ . Since  $\delta_k$  is less than  $\delta_{2k}$ ,  $\delta_{2k}$  should be smaller than  $1/2$  to ensure that the inequality is false, which means at least one nonzero element can be collected. Thus,  $Z_{m1}^t \cap Z_m^t \neq \emptyset$  and the CM operation can work for the reconstruction algorithm if  $\delta_{2k}$  is in  $[0, 1/2]$ .

#### Estimation

There are  $2k$  indices in  $Z_{mi}^t$  in step 3, at least  $k$  of them are not the indices of nonzero elements. The estimation operation is needed to identifying the incorrect indices. We denote the set of correct indices by  $Z_m^t$ . We can define  $\Delta Z = Z_{mi}^t - Z_m^t$  with the estimation set of indices  $Z_{mi}^t$  in step 4. If  $Z_m^t \cap \Delta Z = \emptyset$ , the estimation operation identifies the incorrect indices



successfully, else,  $Z_m^t \cap \Delta Z \neq \emptyset$ , that is, some correct indices are removed by mistake. According to theorem 3 of [18], the reduction of norm introduced by this mistake is proportional to  $\|s_m^t - z_{mi}^t\|_2$  which can be proved to be small. As long as the reduction of the norm is small, a good estimation of  $Z_m^t$  can be obtained.

**Complexity**

The calculation of  $\Phi^* \mathbf{u}_{mi-1}^t$  spends time  $O(LN)$  in step 1, and we can discover the  $k$  largest elements of the  $N$  dimensional vector in time  $O(N \log(N))$  with the quick sort algorithm. In step 2, we can merge two sets of size  $k$  in time  $O(k)$ . In step 3, we multiply both sides of the equation with the  $2k \times 2k$  symmetric positive definite matrix  $\Phi_{Z_{mi}^t}^* \Phi_{Z_{mi}^t}$ , we can get

$$\Phi_{Z_{mi}^t}^* \Phi_{Z_{mi}^t} \mathbf{s}_c = \Phi_{Z_{mi}^t}^* \mathbf{D}_m^t$$

The multiplications spend time  $O(2kL)$ , and the solution  $\mathbf{s}_c$  of the equation can be calculated with the conjugate gradient method with time  $O(4k^2)$ . In step 4, we can discover the  $k$  largest elements of the  $2k$  dimensional vector with time  $O(2k \log(2k))$ , and calculate the residue like step 3 with time  $O(kL)$ . In step 5, we spend time  $O(1)$ . Thus, the total time complexity of one iteration is  $O(LN)$ . According to the convergence conclusion theorem 6 of [18], the iteration number  $n_r$  obeys the following condition.

$$n_r \leq \min\left(\frac{-\log s_{min}}{-\log c_k} + 1, \frac{1.5k}{-\log c_k}\right)$$

where  $s_{min}$  and  $c_k$  are defined as follows.

$$s_{min} = \frac{\min_{1 \leq n \leq N} |s(t, m, n)|}{\|s_m^t\|_2}$$

$$c_k = \frac{2\delta_{3k}(1 + \delta_{3k})}{(1 - \delta^{3k})^3}$$

Consequently, we can get the total time complexity of the reconstruction algorithm  $O(LNn_r)$ .

**4. COLLABORATION IN FUSION CENTER**

We process the set of the measurement vectors  $\{s_m^t, 1 \leq t \leq T\}$  with the decision rule of energy detection to obtain the sensing information

which can show the CR nodes the states of all channels. The decision rule can be written as

$$T(s_{m,n}) = \sum_{t=1}^T |s(t, m, n)|^2 \underset{H_{0,m,n}}{\overset{H_{1,m,n}}{>}} \lambda \tag{12}$$

We can get two important performance parameters associated with spectrum sensing according to equations (4) and (5): the detection probability  $P_{d,m,n}$  and false alarm probability  $P_{f,m,n}$ . Due to channel shadowing and multipath fading, the sensing information of a CR node is usually inaccurate, but the collaboration of multi-nodes can significantly improve the reliability. Let  $Q_{d,n}$  and  $Q_{f,n}$  denote the detection probability and false alarm probability of channel  $n$  after the collaboration, in the conventional algorithm, they can be calculated by

$$Q_{d,n} = 1 - \prod_{m=1}^M (1 - P_{d,m,n})$$

$$Q_{f,n} = 1 - \prod_{m=1}^M (1 - P_{f,m,n})$$

However, the conventional algorithm is not very efficient when the CR nodes are experiencing different fading environments, we introduce weight factor matrix  $W$  to improve its performance, where an entity of the matrix denoted by  $w_{m,n}$  is the weight factor of  $s_{m,n}$ . Here,

$Q_{d,n}$  and  $Q_{f,n}$  can be gotten by

$$Q_{d,n} = 1 - \prod_{m=1}^M w_{m,n} (1 - P_{d,m,n})$$

$$Q_{f,n} = 1 - \prod_{m=1}^M w_{m,n} (1 - P_{f,m,n})$$

An efficient weight factor matrix should be adaptive to the different fading environments, we can update the matrix with historical records. In the initial step  $i = 1$ , we set  $w_{m,n}$  as  $1/N$ , and the collaborative algorithm is conventional. After one sensing procedure, we can update the weight factor matrix by

$$w_{m,n}^{i+1} = \frac{w_{m,n}^i P_{d,m,n}^i}{\sum_{j=1}^M w_{j,n}^i P_{d,j,n}^i}$$

By this update scheme, the CR nodes which can make accurate decision have much contribution to the final decision, the CR nodes which are experiencing deep fading should reduce their influence on the final decision.

**5. SIMULATION RESULTS**



**5.1 Performance Measures**

T. Shensheng and B.L. Mark [19,20] have made lots of work for the performance analysis of spectrum sharing. We can introduce several performance measures highly associated with spectrum sensing from the work of [19], the definitions of these performance measures in the simulation environment are also given to get a better understanding of the numerical results.

**Probabilities of detection, miss detection and false alarm**

The probabilities of detection and false alarm have been defined and denoted by  $Q_d$ ,  $Q_f$  in above sections, respectively. Miss detection probability  $Q_m$  equals  $1 - Q_d$ . In the simulation, they can be given by

$$Q_d = No.correct / (No.correct + No.miss)$$

$$Q_m = No.miss / (No.correct + No.miss)$$

$$Q_f = No.false / (No.correct + No.false)$$

where *No.correct* is the number of successful detections, *No.miss* is the number of miss detections, and *No.false* is the number of false alarms.

**Blocking probabilities**

The call blocking probability of the licensed user denoted by  $P_{b,LU}$ , is defined as the probability that all channels have been occupied by licensed users when a call of licensed user arrives at the channels, the arrival call is blocked.  $P_{b,LU}$  can be given by

$$P_{b,LU} = No.block_{LU} / No.arrival_{LU}$$

where *No.block<sub>LU</sub>* is the number of call blocks of licensed users, and *No.arrival<sub>LU</sub>* is the number of call arrivals of licensed users.

The call blocking probability of the CR node, denoted by  $P_{b,CR}$ , is defined as the probability that all channels have been occupied by licensed users and CR nodes when a call of the CR node arrives at the channels, the arrival call is blocked.

$P_{b,CR}$  can be given by

$$P_{b,CR} = No.block_{CR} / No.arrival_{CR}$$

where *No.block<sub>CR</sub>* is the number of call blocks of CR nodes, and *No.arrival<sub>CR</sub>* is the number of call arrivals of CR nodes.

**Mean reconnection probability**

The mean reconnection probability of CR nodes, denoted by  $P_{r,CR}$ , is defined as the

probability that a call has been blocked due to the overflow of channels and it can reconnect back to the system. The reconnection happens if a channel becomes idle before the waiting time expires.

$P_{r,CR}$  can be given by

$$P_{r,CR} = No.reconnect_{CR} / No.block_{CR}$$

where *No.reconnect<sub>CR</sub>* is the number of reconnections of CR nodes.

**Total channel utilization**

The total channel utilization, denoted by  $\eta$ , is defined as the ratio of the total occupation time of channels to the total simulation time of channels.  $\eta$  can be given by

$$\eta = \frac{\sum_{No.arrival=1}^{max(No.arrival)} t_{wait}^{No.arrival} + t_{residence}^{No.arrival}}{t_{sim} N}$$

where

$t_{sim}$  is the simulation time,

N is the number of channels,

*No.arrival* is the serial number of the call arrivals of both licensed users and CR nodes,

$t_{wait}^{No.arrival}$  is the waiting time of the call *No.arrival*,

$t_{residence}^{No.arrival}$  is the residence time of the call *No.arrival*.

**Mean waiting time of CR calls**

The waiting time of calls of CR nodes consists of two parts. The call waits if it is blocked. The call also waits if a call of the licensed user arrives and chooses the channel occupied by this call. For simplifying the description, we don't give the special notations for these two parts, they are recorded by the simulation program. The mean waiting time of the calls, denoted by  $t_{wait}$ , can be given by

$$t_{wait} = \frac{\sum_{No.arrival_{CR}=1}^{max(No.arrival_{CR})} t_{wait}^{No.arrival_{CR}}}{max(No.arrival_{CR})}$$

**5.2 Numerical Results**

We consider a cognitive radio network within 300×300 meter square area centered at the fusion center, where the arrivals of calls of CR nodes and licensed users are assumed to form independent Poisson processes with rates  $\lambda_1$  and  $\lambda_2$ , respectively. The call holding time of CR nodes and licensed users are assumed to be exponentially distributed with means  $h_1^{-1}$  and  $h_2^{-1}$ , respectively. The residence time of CR nodes and licensed users in the channels are also assumed to

be exponentially distributed with means  $r_1^{-1}$  and  $r_2^{-1}$ , respectively. For testing our algorithm, 300 channels under Rayleigh fading model are chosen to serve the calls of CR nodes and licensed users. In the simulation, the parameters are set as follows:

$\lambda_1$  changes from 1 to 30,  $\lambda_2$  changes from 1 to 20,

$h_1$  equals 0.5,  $h_2$  equals 5,

$r_1$  equals 0.5,  $r_2$  equals 0.2.

The units of  $\{\lambda_1, \lambda_2\}$ ,  $\{h_1, h_2\}$  and  $\{r_1, r_2\}$  are the number of calls / sec, 1 / sec and 1 / sec, respectively.

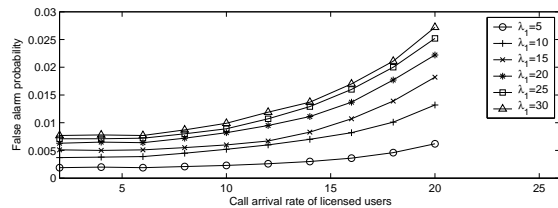
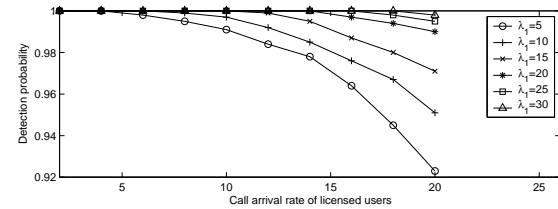


Figure 1: Probabilities of detection and false alarm vs.  $\lambda_2$  for different  $\lambda_1$

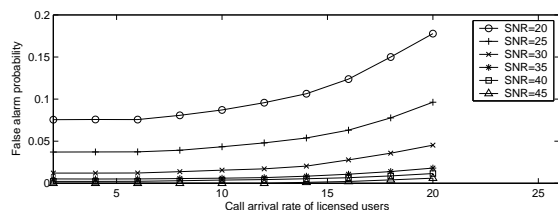
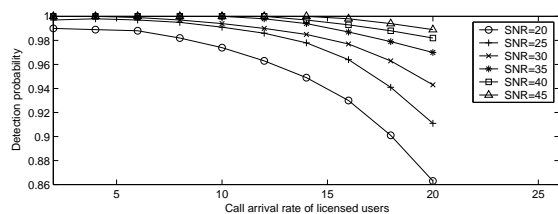


Figure 2: Probabilities of detection and false alarm vs.  $\lambda_2$  at different SNR

The arrival rate of the calls of licensed users  $\lambda_2$  is used as the horizontal axis of the

numerical results for the reason that it determines the sparsity  $k$  of the measurement vector  $\mathbf{s}_m^t$  which has dramatic impact on the performance of our algorithm. We first observe the probabilities of the detection and the false alarm for different arrival rates of CR calls  $\lambda_1$  in Figure 1. We observe that detection probability  $Q_d$  decreases as  $\lambda_2$  increases, and increases as  $\lambda_1$  increases. Meanwhile, the false alarm probability  $Q_f$  decreases as  $\lambda_2$  and  $\lambda_1$  increase. The reasons are that increasing  $\lambda_2$  causes increasing  $k$  which reduces the accuracy of the reconstruction algorithm for  $\mathbf{s}_m^t$ , and the collaboration of CR nodes not only increases  $Q_d$ , but also increases  $Q_f$ . Figure 2 shows  $Q_d$  and  $Q_f$  at different  $\lambda_2$  for different SNR. We observe that  $Q_d$  increases with increasing SNR, and  $Q_f$  decreases with increasing SNR. The reason is that high SNR can make great contribution to the decision of energy detection before the collaboration.

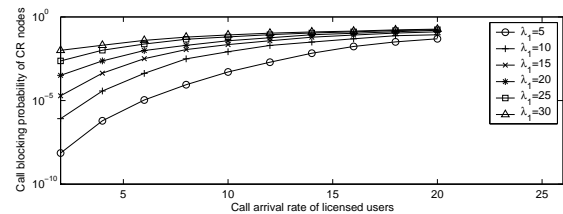
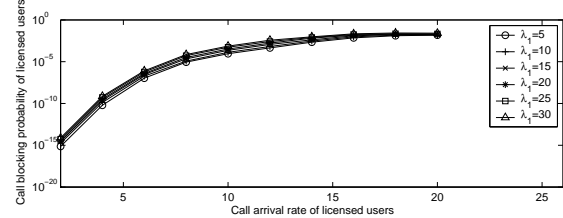


Figure 3: Call blocking probability vs.  $\lambda_2$  for different  $\lambda_1$

We observe that the call blocking probability of licensed users  $P_{b,LU}$  increases with increasing  $\lambda_2$  and doesn't depend on  $\lambda_1$  in Figure 3. Meanwhile, the call blocking probability of CR nodes  $P_{b,CR}$  increases with increasing  $\lambda_2$  and  $\lambda_1$ .

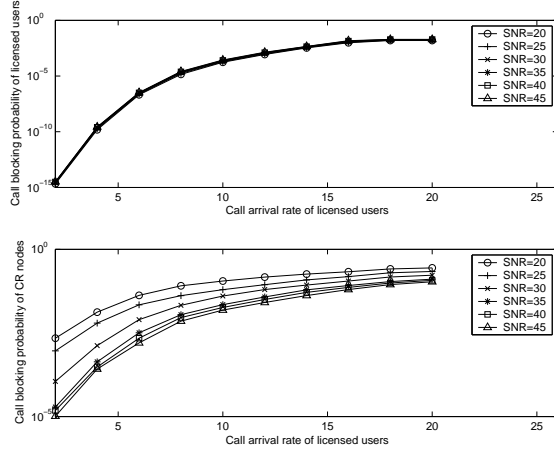


Figure 4: Call blocking probability vs.  $\lambda_2$  at different SNR

The reasons are that the licensed user can select all the channels unoccupied by other licensed users and doesn't know the existence of CR nodes, a call of the licensed user may let a call of a CR node leave one channel. On the other hand, the CR node has to sense the existence of licensed users. We observe that  $P_{b,LU}$  doesn't depend on SNR in Figure 4, and  $P_{b,CR}$  decreases with increasing SNR. The reasons are that  $Q_f$  and the miss detection probability  $Q_m$  decrease as SNR increases according to the observation of Figure 2, and  $P_{b,CR}$  decreases as  $Q_f$  and  $Q_m$  decrease.

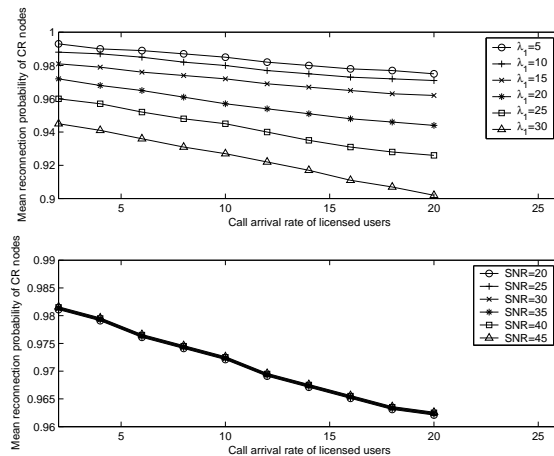


Figure 5: Mean reconnection probability of CR nodes vs.  $\lambda_2$

Figure 5 shows the mean reconnection probability of CR nodes  $P_{r,CR}$ . We observe that

$P_{r,CR}$  decreases as  $\lambda_2$  and  $\lambda_1$  increase. The reasons are that the larger  $\lambda_2$  the more waiting time of CR calls expires, the smaller  $\lambda_1$  the less the number of call blocks  $No.block_{CR}$ . We also observe that  $P_{r,CR}$  doesn't depend on SNR for the reason that  $P_{r,CR}$  doesn't depend on  $Q_f$  and  $Q_m$ .

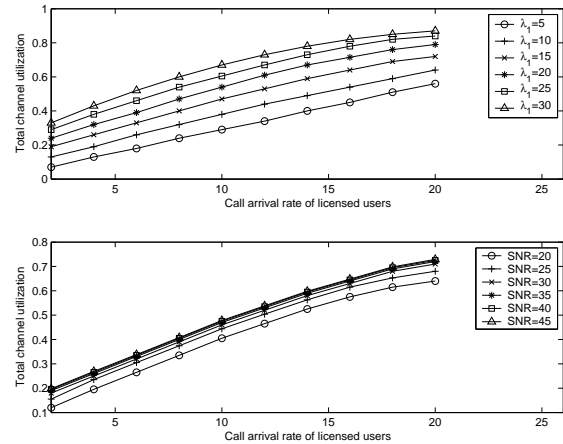


Figure 6: Total channel utilization vs.  $\lambda_2$

Figure 6 shows the total channel utilization  $\eta$ . We observe that  $\eta$  increases as  $\lambda_2$  and  $\lambda_1$  increase. However,  $\eta$  decreases when the sensing information is not very reliable. A channel is wasted when a false alarm event happens. A CR node and a licensed user are affected when a miss detection event happens, and two channels are wasted. Consequently,  $\eta$  decreases when  $Q_f$  increases with increasing  $\lambda_1$ ,  $Q_m$  increases with increasing  $\lambda_2$ . We also observe that  $\eta$  increases as SNR increases for the reason that  $Q_f$  and  $Q_m$  decrease as SNR increases.

Figure 7 shows the mean waiting time of CR calls  $t_{wait}$ . We observe that  $t_{wait}$  increases as  $\lambda_2$  and  $\lambda_1$  increase, and in contrast to Figure 6,  $t_{wait}$  increases when the sensing information is not very reliable, for the reason that false alarm and miss detection events increase the number of CR nodes waiting for the service. We also observe that  $t_{wait}$  decreases as SNR increases for the reason that  $Q_f$  and  $Q_m$  decrease as SNR increases.

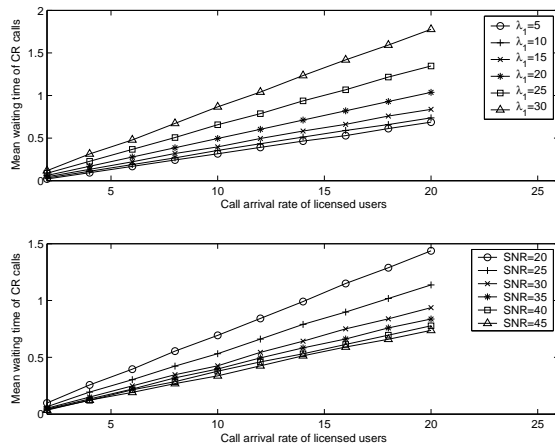


Figure 7: Mean waiting time of CR calls vs.  $\lambda_2$

We observe six performance measures at different call arrival rates of licensed users and CR nodes and different SNR in the system which considers call hold and residence. This simulation can give a comprehensive understanding of the performance of the collaborative wideband sensing algorithm.

## 6. CONCLUSION AND FUTURE WORK

A collaborative wideband sensing algorithm is developed to reduce the time overhead and the communication overhead of the conventional collaborative sensing method. The CR nodes detect linear combinations of the information of all channels in the algorithm, and then transmit the detection vectors to the fusion center where the information of the channels is reconstructed and merged. The sensing procedure in each CR node can be completed in a short time since only a small amount of detection vectors are needed to reconstruct the sensing information of all channels. The sizes of reports are also significantly reduced due to the low dimension of detection vectors. Six performance measures of the algorithm have been evaluated by simulation under the system which considers the call hold and residence of licensed users and CR nodes. Distributed systems are popular in future networks. The distributed collaboration of the sensing information can significantly improve the performance and reliability of the sensing techniques. We will focus on this problem in our future study.

## ACKNOWLEDGMENTS

This work was partly supported by National Natural Science Foundations of P.R. China under grant No.61074033 and No.61233003, Doctoral Fund of Ministry of Education of P.R. China under grant No.20093402110019.

## REFERENCES:

- [1] G. Staple and K. Werbach, The end of spectrum scarcity, *IEEE Spectrum Archive*, Vol. 41, No. 3, 2004, pp. 48-52.
- [2] Shared Spectrum Company, Spectrum Occupancy Report for New York City during the Republican Convention August 30-September 1, 2004, available online at: <http://www.sharespectrum.com/?section=measurements> 2005.
- [3] Q. Zhi, C. Shuguang, H. Poor and A. Sayed, Collaborative wideband sensing for cognitive radios, *IEEE Signal Processing Magazine*, Vol. 25, No. 6, 2008, pp. 60-73.
- [4] V.G. Chavali and C.R.C.M. da Silva, Collaborative Spectrum Sensing Based on a New SNR Estimation and Energy Combining Method, *IEEE Transactions on Vehicular Technology*, Vol. 60, No. 8, 2011, pp. 4024-4029.
- [5] Sang Soo Jeong, Wha Sook Jeon and Dong Geun Jeong, Collaborative Spectrum Sensing for Multiuser Cognitive Radio Systems, *IEEE Transactions on Vehicular Technology*, Vol. 58, No. 5, 2009, pp. 2564-2569.
- [6] C. Yunfei, Optimum number of secondary users in collaborative spectrum sensing considering resources usage efficiency, *IEEE Communications Letters*, Vol. 12, No. 12, 2008, pp. 877-879.
- [7] A.S. Rawat, P. Anand, C. Hao and P.K. Varshney, Collaborative Spectrum Sensing in the Presence of Byzantine Attacks in Cognitive Radio Networks, *IEEE Transactions on Signal Processing*, Vol. 59, No. 2, 2011, pp. 774-786.
- [8] O. Dong-Chan, L. Yong-Hwan, Cooperative spectrum sensing with imperfect feedback channel in the cognitive radio systems, *International Journal of Communication Systems*, Vol. 23, No. 6, 2010, pp. 763-779.
- [9] L. Xin, T. Xuezhi, Optimization algorithm of periodical cooperative spectrum sensing in cognitive radio, *International Journal of Communication Systems*, 2012, DOI: 10.1002/dac.2377.
- [10] C. Hongbin, C. Hsiao-Hwa, Spectrum sensing scheduling for group spectrum sharing in cognitive radio networks, *International Journal of Communication Systems*, Vol. 24, No. 1, 2011, pp. 62-74.
- [11] Z. Qing, T. Lang, S. Ananthram and C. Yunxia, Decentralized cognitive MAC for opportunistic spectrum access in ad hoc networks: A POMDP



- framework, *IEEE Journal on Selected Areas in Communications*, Vol. 25, No. 3, 2007, pp. 589-600.
- [12] S. Ahmad, L. Mingyan, T. Javidi, Z. Qing and B. Krishnamachari, Optimality of Myopic Sensing in Multichannel Opportunistic Access, *IEEE Transactions on Information Theory*, Vol. 55, No. 9, 2009, pp. 4040-4050.
- [13] X. Wang, W. Chen and Z. Cao, Partially observable Markov decision process-based MAC-layer sensing optimisation for cognitive radios exploiting rateless-coded spectrum aggregation, *IET Communications*, Vol. 6, No. 8, 2010, pp. 828-835.
- [14] W. Lingcen, W. Wei and Z. Zhaoyang, A POMDP-based optimal spectrum sensing and access scheme for cognitive radio networks with hardware limitation, *IEEE Wireless Communications and Networking Conference*, 2012, pp. 1281- 1286.
- [15] H. Urkowitz, Energy detection of unknown deterministic signals, *Proceedings of the IEEE*, Vol. 55, No. 4, 1967, pp. 523-531.
- [16] F.F. Digham, M.-S. Alouini and M.K. Simon, On the energy detection of unknown signals over fading channels, *IEEE International Conference on Communications 2003*, pp. 3575-3579.
- [17] E.J. Candes and T. Tao, Decoding by linear programming, *IEEE Transactions on Information Theory*, Vol. 51, No. 12, 2005, pp. 4203-4215.
- [18] D. Wei, O. Milenkovic, Subspace Pursuit for Compressive Sensing Signal Reconstruction, *IEEE Transactions on Information Theory*, Vol. 55, No. 5, 2009, pp. 2230-2249.
- [19] T. Shensheng, B. Mark, Modeling and analysis of opportunistic spectrum sharing with unreliable spectrum sensing, *IEEE Transactions on Wireless Communications*, Vol. 8, No. 4, 2009, pp. 1934-1943.
- [20] T. Shensheng, B. Mark, Analysis of opportunistic spectrum sharing with markovian arrivals and phase-type service, *IEEE Transactions on Wireless Communications*, Vol. 8, No. 6, 2009, pp. 3142-3150.